Risk assessment of forest disturbance by typhoons with heavy precipitation in northern Japan

Junko Morimoto[*,a], Masahiro Aiba[b], Flavio Furukawa[a, d], Yoshio Mishima[c], Nobuhiko Yoshimura[a, d], Sridhara Nayak[e], Tetsuya Takemi[e], Haga Chihiro[f], Takanori Matsui[f], Futoshi Nakamura[a]

[a]Graduate School of Agriculture, Hokkaido University, Sapporo, Hokkaido, 060-8587, Japan

[b]Research Institute for Humanity and Nature, Kyoto, 603-8047, Japan

[c]Faculty of Geo-Environmental Science, Rissho University, Kumagaya, Saitama, Japan

[d]Department of Environmental and Symbiotic Science, Rakuno Gakuen University, Ebetsu 069-8501, Japan

[e]Disaster Prevention Research Institute, Kyoto University, Gokasho, Uji, Kyoto, 611-0011, Japan

[f]Division of Sustainable Energy & Environmental Engineering, Graduate School of Engineering, Osaka University, Suita, Osaka, 565-0871, Japan

***Corresponding author**

Junko MORIMOTO

Graduate School of Agriculture, Hokkaido University, Kita 9, Nishi 9, Kita ku, Sapporo,

Hokkaido, 060-8587, Japan

E-mail: jmo1219@for.agr.hokudai.ac.jp

Tel.: +81-11-736-7735

Author contributions

JM and AM: Conceptualization and methodology; AM, NY, and YM, SN, TT: Software and data curation; JM: Writing - original draft preparation and investigation; AM and FF: Visualization; TT, HC, TM, and FN: Supervision; Everyone: Writing - reviewing and editing

Abstract

Under future climate regimes, the risk of typhoons accompanied by heavy rains is expected to increase. Although the risk of disturbance in forest stands by strong winds has long been of interest, we have little knowledge of how the process is mediated by storms and precipitation. Using machine learning, we assess in cool- temperate forests the disturbance risk by typhoons that landed in northern Japan in late August 2016 to determine the features of damage due to typhoons accompanied by heavy precipitation, discuss how the process is mediated by precipitation as inferred from the modelling results, and delineate the effective solutions for forest management to decrease the future risk in silviculture. In the results, we confirmed two types of behaviours in the model: one represents the same process as that of forest disturbance by the strong wind, which has been widely studied, and another represents a unique process mediated by storms and precipitation, which has not been investigated. Specifically, the ridges that received strong wind from the front side had the highest risk of disturbance. Precipitation increased the probability of disturbance in forest stands, and its effect depended on the dominant species composition. Our hypothesis regarding treefall mediated by storms and precipitation is that rainwater flows into the gaps around the tree root systems during sway, and the introduction of rainwater below the root-soil plate decreases the root anchorage. The species-specific vulnerability to rainfall may depend on the volume of lateral roots. Modelling the disturbance risk helped us to examine the kinds of factors that were related to exposure and vulnerability that should be managed to effectively decrease the risk of disturbance by typhoons during future uncontrollable hazards. It is recommended to avoid silviculture on the ridges of plateaus considering the high risk estimated in this area. In addition, species with dense lateral roots would be suitable for planting because they may have high resistance to typhoons with heavy

precipitation.

Keywords: wind disturbance, risk assessment, topography, total precipitation, forest structure, climate change

1 Introduction

Extremely intense tropical cyclones (categories 4 and 5; maximum wind speed ≥ 69 $m \cdot s^{-1}$) are expected to increase in frequency at the end of the twenty-first century (2075–99) under the Intergovernmental Panel on Climate Change (IPCC) A1B scenario (Murakami et al., 2012). This timescale corresponds to the time when the planted seedlings reach old age and become vulnerable to strong winds in the temperate zone. Tropical cyclones (typhoons) in Eastern Asia sometimes bring heavy rain; Typhoon Morakot in 2009 (over 3000 mm) and Typhoon Talas in 2011 (over 2000 mm) in the western North Pacific region are recent examples that induced extreme rainfall. Several case studies have indicated that precipitation accompanied by a typhoon is expected to be intensified in future climates (for example, Nayak and Takemi, 2019a, 2019b; Takemi, 2019). We should be aware of the increased disaster risk in forest landscapes caused by both strong winds and extreme precipitation in the regions where typhoons are a major natural hazard to forest ecosystems (Nakashizuka, 1989; Yamamoto, 1989).

Risks from climate change impacts result from the interaction of vulnerability, exposure, and hazards (Oppenheimer et al., 2014). In the case of forest damage caused by typhoons, hazards correspond to strong winds and heavy rain, exposure implies the presence of forest ecosystems in places and settings that could be damaged, and vulnerability is the susceptibility of the forest structure to strong winds and heavy rain. All factors related to risk must be considered when analysing the process of emergent risks. Forest disturbance risk models consisting of factors representing hazard, exposure, and vulnerability will also be useful for finding an effective adaptation measure because these models will help us to examine the factors of exposure and vulnerability that will be effective in decreasing the risk under uncontrollable hazards.

Many previous studies have empirically examined windthrow in forest stands and revealed the effects of various factors related to hazards, exposure, and vulnerability. High ridges that run perpendicular to prevailing storm directions protect leeward slopes and valley positions (Kramer et al., 2001). However, when the valley line and wind direction are parallel, the wind will converge along the terrain, and damage will occur along the valley floor (Ruel et al., 1998). The probability of disturbance is also highly dependent on the forest structure. Homogeneous forest stands with trees of the same age, species, and height and with the same arrays have a higher probability of damage than heterogeneous forest stands (Jalkanen and Mattila, 2000; Mitchell et al., 2001; Morimoto et al., 2019), probably because these stands allow strong winds to pass through forest stands while maintaining their high speed.

However, we have little knowledge of how the process of forest disturbance is mediated by storms and heavy rain, which will be a challenge to address under the changing climate. Some studies on forest disturbance in relation to the constant wet condition of soil suggest that shallow rooting depths due to high water tables contribute to the constant high risk of windthrow (Stathers et al., 1994; Mitchell et al., 2001). However, few studies have succeeded in incorporating the ephemeral effect of precipitation into forest disturbance models (Mitchell and Ruel, 2015).

During 14 days in late August 2016, four typhoons crossed Hokkaido, the northern part of Japan, and a total of 9,000 ha of forest was damaged by windthrow and landslides (Bureau of Forestry, Department of Fisheries and Forestry, Hokkaido Government, 2018). The maximum wind speed of over 35 $m \cdot s^{-1}$ was recorded mainly in the southern part of Hokkaido, and the maximum monthly precipitation was updated at 89 points of the 225 meteorological observation points in Hokkaido (Japan Meteorological Agency). These successive typhoons were

accompanied by heavy rainfall and are recognized as a typical example that might frequently occur in the future (Takemi, T., 2019). Then, we built a prediction model to estimate the forest disturbance probability due to typhoons accompanied by heavy rain with hazard, exposure, and vulnerability parameters to (1) identify the features of forest disturbance caused by typhoons accompanied by heavy precipitation, (2) discuss how the disturbance process is mediated by precipitation as inferred from the models and (3) delineate effective solutions in forest management to decrease the risk in silviculture in the future. We used gradient boosted decision trees (GBDTs), a machine learning method, to model the forest disturbance risk.

2 Material and methods

2.1 Study area

Our study focused on 325 km^2 of cool temperate forests in Setana, Hokkaido, Japan (Fig. 1; 41°22.6’N, 139°58’E). This region includes a variety of terrain from flat plains to steep mountains, with altitudes from 0 m to 1300 m. The mean annual temperature in the study area is 8.8 °C, and the mean annual precipitation is 1,055.9 mm (Japan Meteorological Agency; averages for the period 1981–2010). Andosols and brown forest soils were found within the study region, which was dominated by natural forests of *Fagus crenata* Blume, *Betula ermanii* Cham., and *Acer pictum* Thunb. and plantation forests of *Abies sachalinensis* (F. Schmidt) Mast. and *Larix kaempferi* (Lamb.) Carrière.

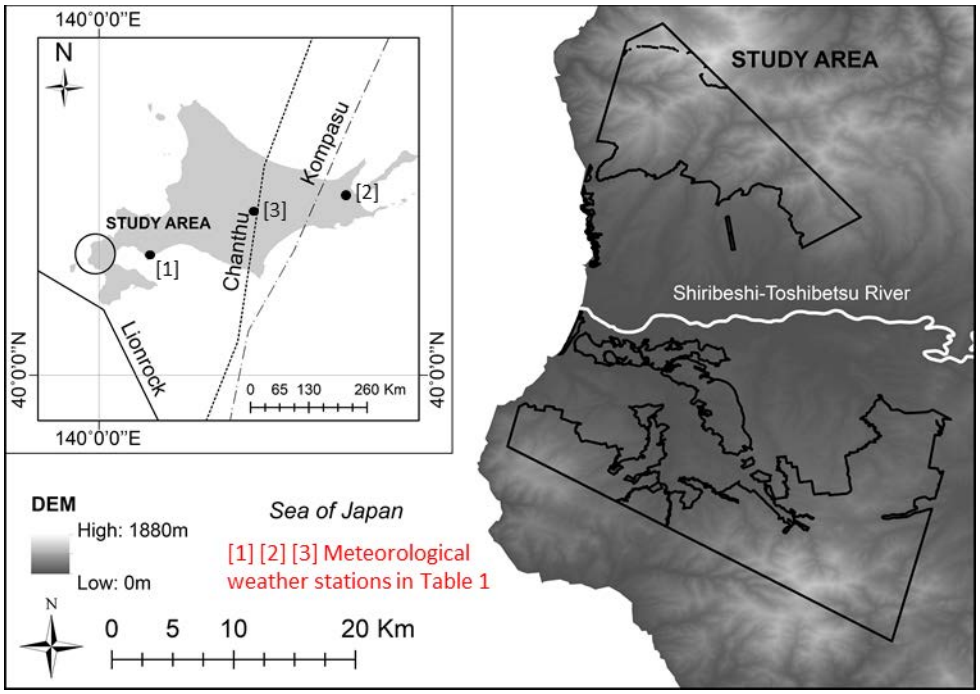

Fig. 1. Study area and tracks of typhoons.

2.2 Typhoons landed in the study area in August 2016

Four typhoons accompanied by heavy precipitation landed on or came close to Hokkaido over the 14 days from August 17th to August 30th (Table 1) and caused significant damage to transportation infrastructure, aquaculture, agriculture, and forestry. Among these typhoons, Chanthu (No. 7, landing on August 17th), Kompasu (No. 11, landing on August 21st), and Lionrock (No. 10, landing on August 30th) affected the study area and caused extensive windthrow and landslides. We focused on the windthrow, especially for the forest collapse which consisted of many fallen trees uprooted and broken trunks without crowns and a few surviving trees. The damage to trees was mostly uprooting, and broken trunks sustained minor damage (uprooted: broken trunks = 7: 3, Supplemental Material S2). The total amount of precipitation over 500 mm was recorded during this period at many meteorological observatories, which is

two to four times greater than the amount of precipitation received in an average year (Japan Meteorological Agency, 2017).

Table 1. General weather conditions during the period of typhoon landing.

Name of typhoon	Typhoon features during landfall			Precipitation accompanied by typhoon			
	Landing period in Hokkaido	Min central pressure (hPa)	Max wind speed (m·s-1)	Precipitation period	Max total precipitation in Hokkaido		
					(mm)	Meteorological weather station recorded [sign on Figure 1]	Location and altitude of the station
Chanthu	Aug. 17th	980	30	Aug. 16-18th	242.5	Nakakineusu [1]	42°13.4'N, 142°56.9'E, 80m
Kompasu	Aug. 21st	994	18	Aug. 20-23rd	296	Itokushibetsu [2]	43°43.3'N, 144°59.3'E, 115m
Linrock	Aug. 30th	940	45	Aug. 26-31st	373	Nukabira [3]	43°22.0'N, 143°11.5'E, 540m

The record is cited from the report by the Japan Meteorological Agency (2016).

2.3 Windthrow mapping

PlanetScope satellite imagery (Planet Lab Inc., 2020) was used for windthrown mapping. The satellites deliver images with a spatial resolution of 3 m per pixel in four different spectral bands: blue (455 – 515 nm), green (500 – 590 nm), Red (590 – 670 nm), and near infrared (780 – 860 nm). The temporal resolution was approximately daily with a constellation operation of more than 130 satellites, which was crucial for vegetation change detection analysis (Guangxing Wang, 2013). We used the Level3B product, which was already orthorectified and radiometrically calibrated to surface reflectance. Before the study, we ensured that windthrown areas could be identified in the PlanetScope satellite imagery (Supplementary material S1). We used pre-typhoon images collected on June 28th and July 1st, 2016, depending on the region, and post-typhoon images collected on September 21, 2016, through the PlanetScope platform. The images pre- and post-typhoons were individually combined to cover the study area.

The spectral angle mapper (SAM) algorithm was used to detect windthrow areas. The SAM is a spectral classification algorithm that calculates the spectral similarity based on the

157 spectral angle between pixels of an input image and training samples (Kruse et al., 1993). First,
158 we created an input image that has ten spectral bands by layer stacking the spectral bands from
159 the pre-typhoon (4 bands) and post-typhoon (4 bands) images plus normalized difference
160 vegetation index (NDVI) bands calculated from each image (2 bands). Windthrown areas should
161 have their specific spectral characteristics in the input image (Coppin and Bauer, 1996). Next, we
162 created training samples of windthrown areas through visual interpretation comparing the post-
163 typhoon image with the pre-typhoon image. These images were created in obvious windthrown
164 areas. Finally, we detected windthrown areas using the input image and training samples through
165 the SAM algorithm on the Semi-Automatic Classification Plugin (Congedo, 2016) within QGIS
166 3.02 (QGIS.org, 2020) (Supplementary material S1). With the SAM method, there is a possibility
167 that land use with spectral characteristics remarkably similar to a windthrow, such as grassland,
168 will be erroneously classified to be windthrow. However, since our methods use the spectral
169 features before and after the typhoons for the classification, such a probability is rare.
170 The test data for accuracy assessment of the windthrow mapping were created using 100
171 random samplings, which were visually interpreted in the same way as the training sample. In
172 addition, the post-typhoon WorldView2 imagery (August 20th, 2017), which provides a higher
173 spatial resolution of 0.37 cm/px, was used as a reference image. The assessment results of the
174 accuracy of the windthrow mapping revealed a substantial level of agreement (kappa = 0.8,
175 overall accuracy in the confusion matrix = 90 %). The total windthrow area within the study
176 region was approximately 240 ha, with a mean patch size of 0.038 ha (maximum = 7.16 ha,
177 minimum = 0.01 ha).
178
179 ***2.4 Preparing the dataset for modelling***

The study area of 325 km^2 was divided into 10 m × 10 m grid cells using geographic information systems. For modelling, all 16,472 positive (forest disturbance) cases and 49,416 randomly sampled (three-fold of the positive cases) negative cases were used. The estimated value of the probability by modelling did not indicate the actual probability of forest disturbance at this event but rather its relative probability. As for explanatory variables, we firstly selected the crucial factors identified by previous studies focused on windthrow risk assessments in mountainous region dominated by cool-temperate and boreal forests (Kramer et al., 2001; Mitchell et al., 2001; Nakajima et al., 2009). In addition to it, we selected series of precipitation indicators identified by previous study focusing on shallow landslide in forests by heavy rainfall (Dou et al., 2019). After the preliminary analyses, variables whose contributions were limited were omitted from the final model for ease of interpretation. Then seventeen explanatory variables were considered in this study as follows: meteorological hazard factors (n = 6): maximum wind speed of typhoon Mindulle ($m \cdot s^{-1}$), maximum wind speed of typhoon Linrock ($m \cdot s^{-1}$), duration of wind speed ≥ 15 $m \cdot s^{-1}$ during typhoon Linrock ($m \cdot s^{-1}$), maximum wind speed of typhoon Chanthu ($m \cdot s^{-1}$), duration of wind speed ≥ 15 $m \cdot s^{-1}$ during typhoon Chanthu ($m \cdot s^{-1}$), and total rainfall during the typhoon period (mm); topographical exposure factors (n = 6): surface geology type, slope angle (°), topex (topographic exposure index, Miller et al., 1987; explained later) with a 1 km line length, topex with a 2 km line length, topex with a 3 km line length, and the slope direction relative to the wind of the highest speed (°, 0=head on, 180=opposite); and forest vulnerability factors (n = 5): forest type (planted or natural), stand age (years), mean diameter at breast height (DBH) of the dominant species (cm), dominant forest species of the forest stand) and stand volume per 100 m^2 (m^3).

For the calculation of the maximum wind speed and the duration of wind speed ≥ 15 $m \cdot s^{-1}$ of typhoons Chanthu, Kompasu, and Linrock, the Advanced Research Weather Research and Forecasting (WRF) model (Skamarock et al., 2008) with two-way configuration and four nested domains with 9 km, 3 km, 1 km and 200 m resolutions was used to numerically simulate the three typhoons and the surrounding meteorological fields. The criterion of wind speed ≥ 15 $m \cdot s^{-1}$ is the threshold of strong winds due to typhoons by the Japan Meteorological Agency (JMA) definition, which is slightly lower than the threshold 17.2 $m \cdot s^{-1}$ of tropical storms by World Meteorological Agency (WMA) definition. The meteorological simulations for typhoon Chanthu and typhoon Lionrock were conducted by Nayak and Takemi (2019a, 2019b). The same model configurations used in Nayak and Takemi (2019a, 2019b) were integrated in this study but with four nested domains. Takemi (2018) used a horizontal grid spacing of 167 m to simulate the heavy rainfall event that occurred in the northern part of Kyushu Island in July 2017 and indicated that the 167-m grid simulation quantitatively captured the rainfall amount. Takemi and Ito (2020) examined the ability to represent strong winds due to typhoons in complex terrain with a horizontal grid spacing of 200 m and indicated that the wind speeds simulated with a grid spacing of 200 m were quantitatively estimated better than those simulated with a grid spacing of 1 km. In this way, both studies demonstrated that the grid spacing on the order of 100 m adequately captured the spatial and temporal variability of rainfall and wind in complex terrain. In this study, we took advantage of high-resolution simulations with a grid spacing on the order of 100 m. The initial and boundary conditions for the WRF simulations were provided from the Japanese Reanalysis (JRA55) dataset. For the calculation of precipitation, the 1-km Radar-AMeDAS precipitation data were downscaled to 200 m resolution by using the nearest neighbour interpolation technique with the help of CDO (Climate Data Operators) software

(CDO, 2019). The interpolation was based on the YAC (Yet Another Coupler) software package (Hanke et al., 2016).

Topex (Miller et al., 1987) and slope angle were calculated using a digital elevation model with a 10-m resolution (Geospatial Information Authority of Japan) by QGIS2.18.26 (QGIS Development Team, 2018) and GRASS7.4.3 (GRASS Development Team, 2018). Slope angle under 5º corresponds to 9 % in slope steepness meaning gentle, the slope angle over 35º corresponds to 70% in slope steepness meaning steep slope, between 5 º and 35 º corresponds to between 9 % and 70% meaning moderate and strong slope. The distance-limited topex is the sum of the elevation angles (above the horizon) or depression angles (below the horizon) estimated at specified intervals on straight lines radiating outward from the target point in eight directions. A positive topex value indicates sheltered topography (valley), a value of 0 indicates a flat plain, and a negative value indicates exposed topography (ridge). We used line lengths of 1, 2, and 3 km, with measurement intervals of 100 m based on Lanquaye-Opoku and Mitchell (2005) and Mitchell et al. (2001). Forest stand features immediately before the typhoons were derived from the forest inventory data investigated in 2013 (Hokkaido Regional Forest Office).

2.5 Modelling and validation

Forest disturbance by typhoons was modelled as a function of the 17 explanatory variables described above and 2 spatial variables (i.e., latitude and longitude) using GBDTs. Spatial variables were included in the model to capture spatial autocorrelations that were not explained by other variables.

The machine learning method is a powerful tool for variable selection, and it is particularly suited to handling prediction problems that include nonlinear relationships between

predictor and response variables and complex interactions between variables (Sandri and Zuccolotto, 2006; Strobl et al., 2007). Gradient boosting is an ensemble learning method that sequentially combines multiple weak learners (in our case, decision trees) that are developed with gradual emphasis on observations poorly predicted by the current ensemble model. This technique permits the development of a model with a high predictive performance without overfitting, in which high dimensional interactions among explanatory variables and nonlinear responses are fully accounted for. Interpretation of GBDTs is not as simple as conventional methods such as generalized linear models, but several techniques, including individual conditional expectation (ICE) plots and Friedman's H statistics, have recently been developed to compensate for these shortcomings. According to these advantages, in forestry, gradient boosting has been frequently used for modelling stand volume (Dube et al., 2015), canopy cover (Freeman et al., 2015), and species distribution (Elith et al. 2008).

The following candidate values were tested for the GBDT models: 3, 5, and 10 for the maximum depth of variable interactions for each learner; 5, 10, and 20 for the minimum number of observations in the terminal nodes for each learner; 0.5 and 0.8 for the proportion of training data used to build each learner; and 400, 600 and 800 for the total number of learners. The shrinkage parameter was set to 0.01 during model assembly. The optimal parameters were determined using spatially blocked 10-fold cross validation, and model predictive performance was evaluated using Matthew's correlation coefficient (MCC) for the optimum threshold. Accuracy and AUC were also calculated, although the optimal parameter was determined using MCC.

The relative importance of explanatory variables was evaluated as a decrease in MCC after permutation of a variable (Breiman, 2001). The average and context-dependent effects of

each explanatory variable on the probability of forest disturbance were visually inspected by a partial dependence plot (Friedman, 2001) and ICE plot (Goldstein et al., 2015), respectively. The ICE plot visualizes the effect of a given explanatory variable for each observation by connecting the outcome of a model while shifting the values of the focal explanatory variable throughout the range while keeping other explanatory variables as the original value. The partial dependence plot indicates the average trend of each curve in the ICE plot. For the ICE plot, each line was centred at zero at the left end of the x-axis to show the relative effects of explanatory variables (c-ICE plot *sensu* (Goldstein et al., 2015)). Each line in the ICE plot was coloured based on the value of the second explanatory variable to assist with the assessment of the interactive effects of the two predictors. Friedman's H statistic (Friedman and Popescu, 2008) was used to detect explanatory variables whose interaction with the vegetation variables was important and therefore should be used for colour-coding of an ICE plot. Friedman's H is defined as a proportion of the variance in partial dependence estimates explained by interactive effects for arbitrary suites of explanatory variables. Three hundred sites were randomly sampled for the ICE plot to prevent the plots from being too dense.

3 Results

Most of the model performance indices (MCC=0.70, AUC=0.92, Accuracy=0.89) were reasonably high compared with those of previous studies (Hanewinkel et al., 2004: MCC=0.16-0.20, accuracy=0.65-0.70, Morimoto et al., 2019: MCC=0.28, AUC=0.93, accuracy=0.88).

Fig. 2 shows the importance of the predictor variables from gradient boosting for predicting forest disturbance by typhoons. The three most important variables excluding spatial variables that were influential on the forest disturbance were dominant species, relative slope

direction, and total precipitation. The maximum wind speed itself had low importance on the prediction because it was highly correlated with topex (3 km) (Spearman's rho = -0.42), which was ranked as the 6th most important variable for predicting the forest disturbance. Topex (3 km) has two effects on forest disturbance: one is the sidelong effect that appears through the maximum wind speed (the wind speed is higher in ridges; therefore, forest disturbance risk rises there), and the other is the sheer effect of topography represented by topex (3 km) (strong winds blow through while keeping the wind speed at the ridge, and turbulence occurs at the leeward side of the ridge; therefore, forest disturbance is more likely to occur on the side than in the valleys and slopes that experienced the same wind speed). Topex (3 km), which can explain both the effects of wind speed and topography, is more likely to be selected as an effective variable than the maximum wind speed. Once topex (3 km) is selected, the maximum wind speed alone does not have much influence on the forest disturbance.

When we discuss the effect of a factor, we should consider its interaction with other factors. Friedman's H, which indicates the strength of an interactive effect with other variables, was high for dominant species, relative slope direction, and total precipitation (Fig. 3a), which all have relatively high variable importance (Fig. 2). Dominant species moderately interacted with total precipitation (Fig. 3b), and the relative slope direction moderately interacted with dominant species (Fig. 3c) because the proportion of the variance explained by the interactive effects was approximately 0.25 to 0.3.

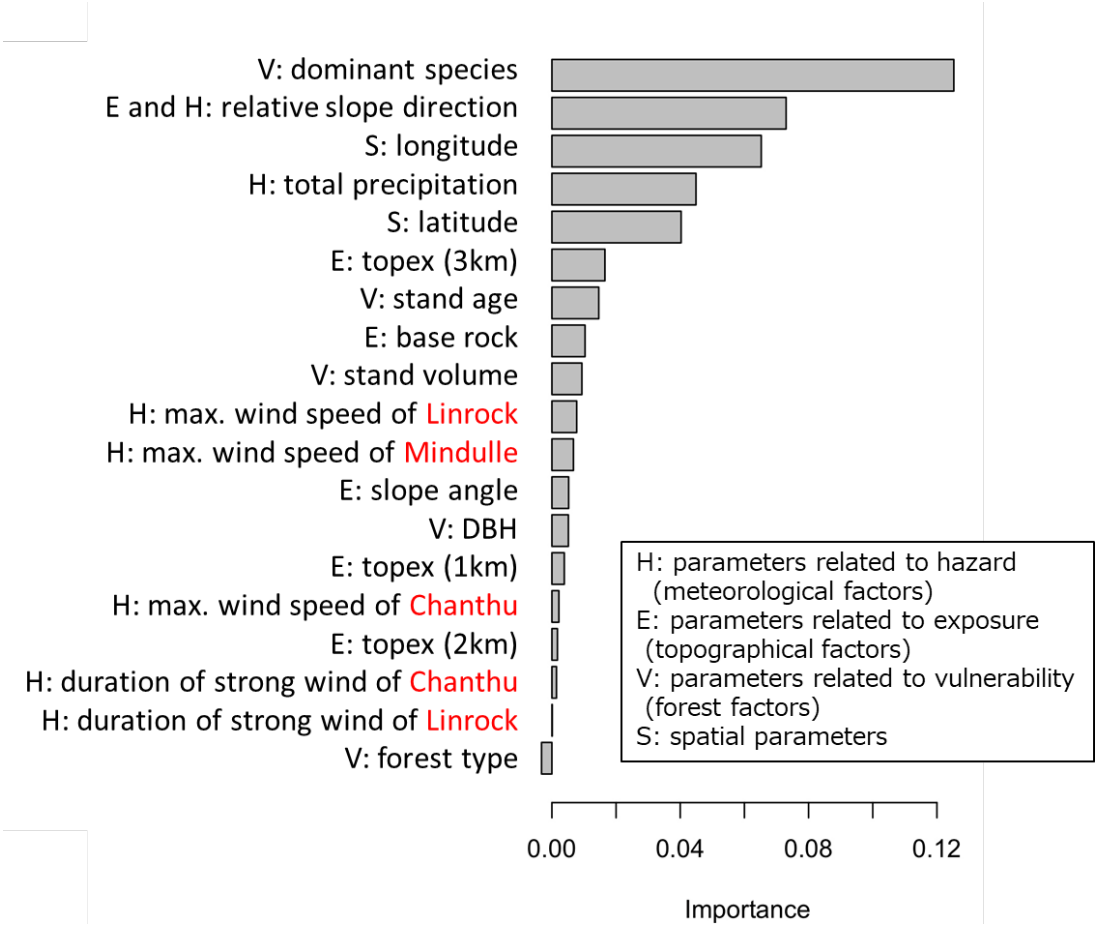

314

315

316 **Fig. 2.** Variable importance plots for predictor variables from gradient boosting for predicting the

317 forest disturbance by typhoons.

318

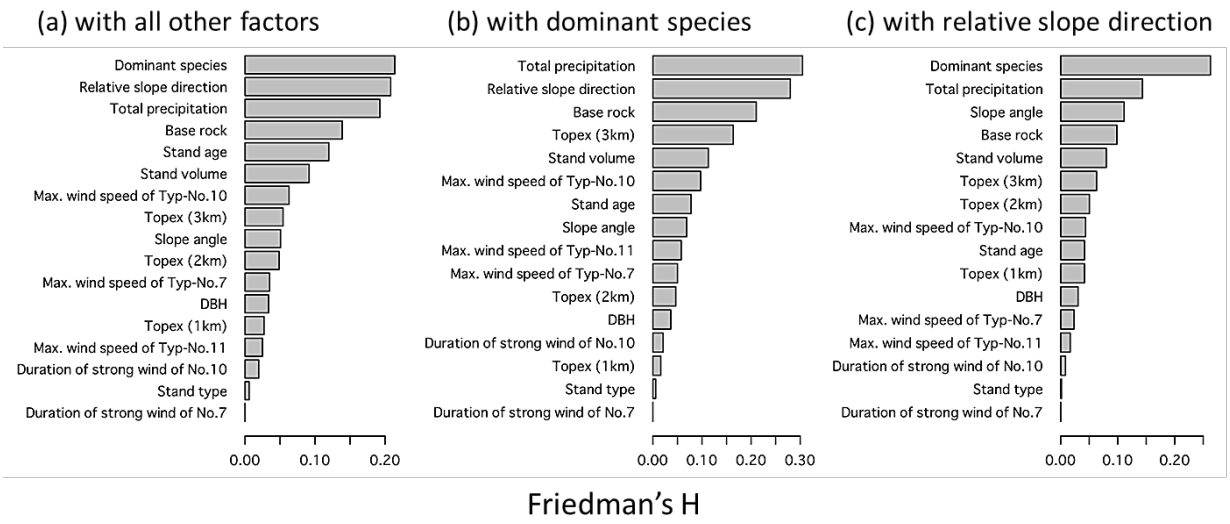

Fig. 3. Friedman's H-statistics of each factor (a) with all other factors, (b) with dominant species, and (c) with relative slope direction for a model predicting the forest disturbance probability.

The partial plot showed the highest probability of disturbance in the *A. sachalinensis* stand among the main stands of five dominant species in the study area when other variables were fixed (Fig. 3a). A strong wind blowing from the front side of the slope showed a high probability of disturbance, regardless of the angle (Fig. 3b). The closer the wind direction was to the back of the slope, the lower the risk of disturbance. The probability of forest disturbance increased in stages when the total precipitation reached 60 mm and 100 mm (Fig. 4c). The probability of forest disturbance was higher in the ridge than in the flat and valley zones at the topography scale of 3 km (Fig. 4d).

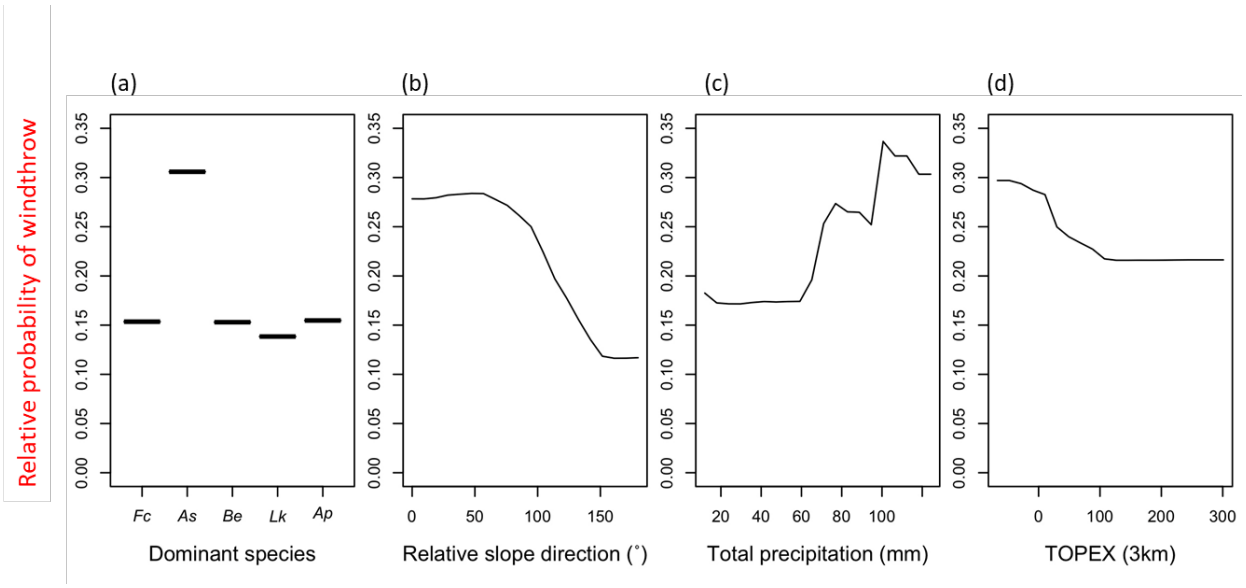

Fig. 4. Partial dependence plots for major predictor variables for GBDT predictions of forest disturbance occurrence; (a) dominant species (Fc (*Fagus crenata*), As (*Abies sachalinensis*), Be (*Betula ermanii*), Lk (*Larix kaempferi*), Ap (*Acer pictum*)), (b) relative slope direction (°), (c) total rainfall (mm), and (d) topex (3 km). Each plot is drawn in only the range or ranges of the subsample used for modelling.

The increasing pattern of the forest disturbance probability associated with the increasing total precipitation was different depending on the dominant species of the stands (Fig. 5). The disturbance probability of *A. sachalinensis* stands increased sharply when the total rainfall exceeded 60 mm. The stands of other dominant species showed a lower disturbance probability than *A. sachalinensis* stands in the total precipitation stage from 60 mm to 80 mm. Although sharp increases in disturbance probability were also observed for other species when total rainfall was > 100 mm, these responses are not very reliable or applicable due to the limited number of sites that experienced such high rainfall.

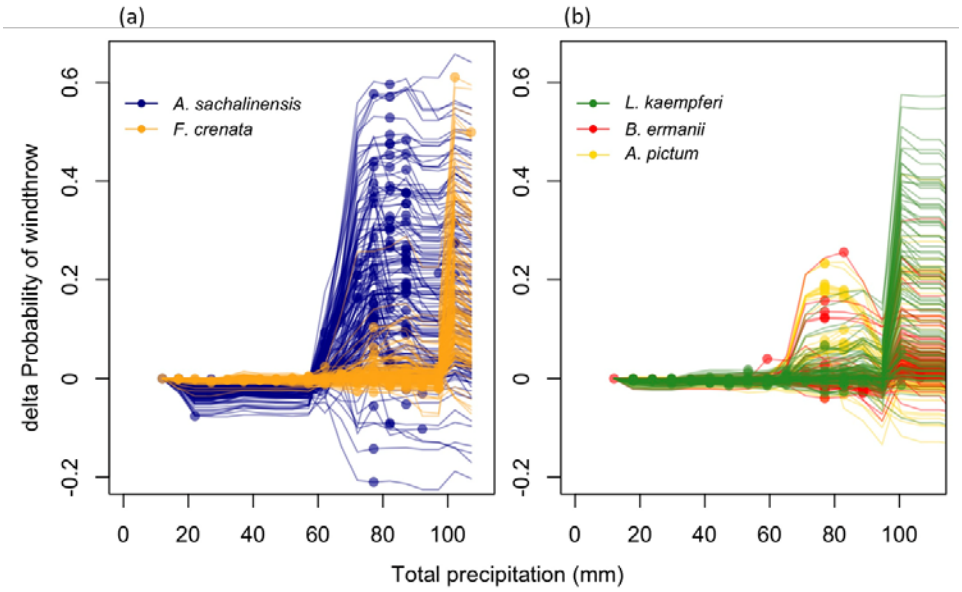

345

346 **Fig. 5.** Mutual effects between species and total precipitation on the probability of forest
347 disturbance. (a) *A. sachalinensis* and *F. crenata;* (b) *A. pictum, B. ermanii,* and *L. kaempferi.*
348 Expected responses for each grid were centred at zero at the low end of an explanatory variable.
349 Filled circles indicate observed values of an explanatory variable for each site. Three hundred
350 sites were randomly sampled for visualization to prevent the plots from being too dense.

351

352 **4 Discussion**

353

354 ***4.1 Feature of forest disturbance by typhoon accompanied by heavy precipitation***

355 We confirmed two types of behaviours of the model: one represents the same process as that of
356 forest disturbance by strong wind, which has been widely studied, and another represents a
357 unique process mediated by storms and precipitation, which has not been investigated. The
358 former type of forest disturbance can occur in the early periods of typhoon landing and the latter
359 type of forest disturbance can occur in the late periods because the cumulative rainfall increases
360 as time passes.

Ridges exhibited a high risk of forest disturbance (Fig. 4d), as indicated in many previous studies (Everham and Brokaw, 1996; Kramer et al., 2001), suggesting that strong winds predominantly blew across valleys and caused stronger wind speeds at ridges than valleys (Ruel et al., 1998) during typhoon landings. The effects of topography on the forest disturbance probability actually included the effects of maximum wind speed, as a strong correlation was indicated between topex (3k) and maximum wind speed. In addition, the decreasing pattern of forest disturbance probability along with the increasing relative slope direction (Fig. 4b) explained the contrasting damages across ridges due to the high variety of combinations in the direction of the strong wind and the slope aspect in mountainous landscapes (Rentch, 2010). Our analysis more specifically explained the old assertion that local unique topography increases the probability of windthrow due to complex terrain (Ruel et al., 1998; Kramer et al., 2001).

Precipitation was shown to increase the risk of forest disturbance in forest stands, and its effect was dependent on the dominant species of the stands. Total precipitation over 60 mm during typhoon periods highly contributed to the forest disturbance (Fig. 2, Fig. 4c). Although not all the total rainfall penetrated the soil and contributed to uprooting, it suggests that there was some correlation with the amount of rainfall that substantially contributed to uprooting. This result corresponds to a previous report that stated that tree stability was lower after rainfall (1 day after 68 mm of precipitation along with a typhoon) than before (Koizumi, 1987), which was confirmed by the tree-pulling test for five trees. In general, uniform structured forests such as plantations are more vulnerable to storms than are multistoried natural forests (Quine and Gardiner, 2007; Morimoto et al., 2019). However, the effect of the dominant species was more important than that of the forest type (plantation or natural) in our model, suggesting that the tree form representing the species features controls the process of forest disturbance in the case of

384 rain typhoons.

385 In general, thick and long taproots have the effect of anchor, avoiding from uprooting
386 (Karizumi, 2010). However, the anchor effect was not exerted under the rainy typhoon, given *A.*
387 *sachalinensis* whose taproot highly developed (Supplementary material S3) uprooted at lower
388 level of precipitation than other species. Interestingly, *A. sachalinensis* has a higher tendency in
389 uprooting by strong wind from the perspective of physical structure in root systems and canopy
390 traits (Supplementary material S3) showed high vulnerability to precipitation (Fig. 5); other
391 species that have a lower tendency in uprooting from the perspective of physical structure
392 showed mostly high resistance to precipitation. In particular, we noticed a lower density of
393 lateral and fine roots in *A. sachalinensis* than in other species. This result corresponded to the
394 previous suggestions that the horizontal distribution of root systems should serve as the major
395 resistance to windthrow (Krause et al., 2014), and few large trees can rely solely on tap roots and
396 need to develop thick lateral roots to prevent uprooting (Crook and Ennos, 1998).

397 The allometry of tree height with respect to the trunk diameter (height/DBH) has been
398 discussed as one of the most important factors determining windthrow damage (Cremer et al.,
399 1982; Ancelin et al., 2004). This parameter in the present study area ranged from 54 to 86 and 53
400 to 83 for *A. sachalinensis* and *L. kaempferi*, respectively. These ranges indicate the windthrow
401 risk from low to high according to Shibuya et al. (2011). Moreover, the ranges of allometry
402 values were similar for the two species, meaning that this factor cannot explain the difference in
403 vulnerability to precipitation, although this is one of the factors often related to treefalls by
404 typhoons.

405

406 ***4.2 Hypothesis of the forest disturbance process mediated by storm and precipitation***

The general process of treefall elucidated by tree-pulling experiments (Coutts, 1986; Karizumi, 2010; Kamimura et al., 2012) and the shapes of the root system related to resistance to windthrow (Krause et al., 2014) provide us with the opportunity to form a hypothesis on how the forest disturbance process is mediated by storms and precipitation inferred from the modelling results. We focused on the process of uprooting because it was the dominant type of damage after the events, and it has been reported that uprooting was identified under wet conditions more than stem snapping when 16 studies of wind disturbance were compared (Peterson and Pickett, 1991).

Three types of interspaces will emerge in the soil around tree root systems when a tree is attacked by strong wind (Supplementary Material S4a): the first is a small hollow hole between roots and the adhering soil (Karizumi, 2010), the second is a complex network of cracks developed on the windward edge of the root-soil plate, and the third is an irregular crack that appears under the root-soil plate, apparently as a result of stretching the undersurface of the plate and separation of the sinker roots (Coutts, 1986). Rainwater penetrates all of these gaps and ultimately contributes to increasing the water content below the root-soil plate. The water content below the root plate significantly affects root anchorage, i.e., high water content below the root plate decreases root anchorage (Kamimura et al., 2012), which will then cause the tree to fall over. The difference in vulnerability to rainfall may stem from the shape of the root system, especially the volume of lateral roots, which serves as the major resistance to uprooting (Krause et al., 2014). Dense lateral roots and fine roots will be able to widely disperse rainwater inside the soil-root plate and postpone rainwater pooling under the plate. However, sparse lateral roots and fine roots with thick taproots may gather most of the rainwater into cracks formed just below the taproot, and the water content under the root plate may rise immediately (Supplementary Material S4a). The root system of *A. sachalinensis* (Supplementary Material S4b), which had a

physical structure that was more likely to be uprooted by strong winds than other tree species, also had root systems in which the soil water content under the root plate easily increased by heavy rain (Supplementary Material S4b). Therefore, the difference among species in the risk of forest disturbance appeared clearly.

This hypothesis should be verified by future tree-pulling experiments under artificial rain and modelling the tree behaviour under storm and rain conditions.

4.3 Effective solutions in forest management to decrease the risk in silviculture

Forest disturbance risk modelling comprised of three main drivers (Oppenheimer et al., 2014) helps us to examine what kind of factors related to exposure and vulnerability are to be managed to effectively decrease the risk in silviculture in the situation of uncontrollable hazards in the future. Regarding controlling exposure, avoiding silviculture on a ridge is recommended considering that the risk estimated in this area was higher not only in our study but also in many previous windthrow models (for example, Mitchell, 2013). In addition to controlling exposure, vulnerability control is also important. In our model, dominant tree species were related to forest disturbance through vulnerability to rainfall. Species having dense lateral roots would be suitable for planting because they may have higher resistance to typhoons accompanied by heavy rain. However, we must admit the limitation of our analyses. Our modelling only expresses the pattern or process that a major trend shows because all variables are simulated or estimated. Then, we cannot discuss the minor trend of forest disturbance. Additionally, the high importance of latitude and longitude in our model (Fig. 2) means that there are still missing spatial variables that are strongly related to forest disturbance by typhoons, although we tried to include all the possible factors we could evaluate. We might determine a more specific process of forest disturbance by

typhoons accompanied by heavy precipitation after including new principal parameters.

Acknowledgements

We appreciate Hokkaido Regional Forest Office of Forestry Agency and Hokkaido Government's Bureau of Forestry for providing the forest inventory.

Funding

This study was supported by the JSPS KAKENHI Grant Number JP 17H01516, S-15 PANCES of the Ministry of the Environment, Japan, the Integrated Research Program for Advancing Climate Models (TOUGOU) Grant Number JPMXD0717935498 from the Ministry of Education, Culture, Sports, Science and Technology (MEXT), Japan.

Role of the funding source

In study design and data collection

Declarations of interest

None

Data availability

The datasets presented in this article are not readily available because they contain forest inventory data restricted by the Hokkaido Regional Forest Office of Forestry Agency and

Hokkaido Government’s Bureau of Forestry. Requests to access the datasets should be directed to Junko Morimoto.

References

Ancelin, P., Courbaud, B., Fourcaud, T., 2004. Development of an individual tree-based mechanical model to predict wind damage within forest stands. For. Ecol. Manag. 203, 101–121. https://doi.org/10.1016/j.foreco.2004.07.067.

Bureau of Forestry, Department of Fisheries and Forestry, Hokkaido Government, 2018. Growing forests to reduce the risk of damage of windthrow. 8pp. in Japanese. http://www.pref.hokkaido.lg.jp/sr/srs/riskdown.pdf.

Busgen, M., Munch, E., 1929. The structure and life of forest trees, Chapman and Hall Limited, London, UK.

Breiman, L., 2001. Random forests. Mach. Learn. 45, 5–32. https://doi.org/10.1023/A:1010933404324.

Congedo, L., 2016. Semi-Automatic Classification Plugin Documentation. https://doi.org/10.13140/RG.2.2.29474.02242/1.

Coppin, P.R., Bauer, M.E., 1996. Digital Change Detection in Forest Ecosystems with Remote Sensing Imagery. Remote Sens. Rev. 13, 207–234. https://doi.org/10.1080/02757259609532305.

Guangxing Wang, Q.W., 2013. Remote Sensing of Natural Resources, 1st ed. Taylor & Francis.

Coutts, M.P., 1986. Components of tree stability in sitka spruce on peaty gley soil. For. Int. J. For. Res. 59, 173–197. https://doi.org/10.1093/forestry/59.2.173.

Cremer, K.W., Borough, C.J., McKinnell, F.H., Carter, P.R., 1982. Effects of stocking and thinning on wind damage in plantations. N. Z. J. For. Sci. 12, 244–268.

Crook, M.J., Ennos, A.R., 1998. The increase in anchorage with tree size of the tropical tap rooted tree mallotus wrayi , king (*Euphorbiaceae*). Ann. Bot. 82, 291–296.

https://doi.org/10.1006/anbo.1998.0678.

Dou, J., Yunus, A. P., Xu, Y., Zhu, Z., Chen, C., Sahana, M., Khosravi, K., Yang, Y., Pham, B. T., 2019. Torrential rainfall-triggered shallow landslide characteristics and susceptibility assessment using ensemble data-driven models in the Dongjiang Reservoir Watershed, China, Natural Hazards. 97:579–609. https://doi.org/10.1007/s11069-019-03659-4.

Dube, T., Mutanga, O., Abdel-Rahman, E.M., Ismail, R., Slotow, R., 2015. Predicting Eucalyptus spp. stand volume in Zululand, South Africa: an analysis using a stochastic gradient boosting regression ensemble with multi-source data sets. International Journal of Remote Sensing. 36:14, 3751-3772, DOI: 10.1080/01431161.2015.1070316.

Elith, J., Leathwick, J.R., Hastie, T., 2008. A working guide to boosted regression trees. J Anim Ecol. 77, 802–813. https://doi.org/10.1111/j.1365-2656.2008.01390.x.

Everham, E.M., Brokaw, N.V.L., 1996. Forest damage and recovery from catastrophic wind. Bot. Rev. 62, 113–185. https://doi.org/10.1007/BF02857920.

Freeman, E.A., Moisen, G.G., Coulston, J.W., Wilson, B.T., 2015. Random forests and stochastic gradient boosting for predicting tree canopy cover: comparing tuning processes and model performance. dx.doi.org/10.1139/cjfr-2014-0562.

Friedman, J.H., 2001. Greedy function approximation: a gradient boosting machine. Ann. Stat. 29, 1189–1232. https://doi.org/10.1214/aos/1013203451.

Friedman, J.H., Popescu, B.E., 2008. Predictive learning via rule ensembles. Ann. Appl. Stat. 2, 916–954. https://doi.org/10.1214/07-AOAS148.

Goldstein, A., Kapelner, A., Bleich, J., Pitkin, E., 2015. Peeking inside the black box: visualizing statistical learning with plots of individual conditional expectation. J. Comput. Graph. Stat. 24, 44–65. https://doi.org/10.1080/10618600.2014.907095.

GRASS Development Team, 2018. Geographic Resources Analysis Support System (GRASS) software. Open Source Geospatial Foundation. http://grass.osgeo.org/(accessed 29 May 2020).

Hanewinkel, M., Kuhn, T., Bugmann, H., Lanz, A. Brang, P., 2014. Vulnerability of uneven-aged forests to storm damage. Forestry. 87:4, 525–534. doi:10.1093/forestry/cpu008.

Hanke, M., Redler, R., Holfeld, T., Yastremsky, M., 2016. YAC 1.2. 0: new aspects for coupling software in earth system modelling. Geosci. Model Dev. 9, 2755–2769. https://doi.org/10.5194/gmd-9-2755-2016.

Jalkanen, A., Mattila, U., 2000. Logistic regression models for wind and snow damage in northern Finland based on the national forest inventory data. For. Ecol. Manag. 135, 315–330. https://doi.org/10.1016/S0378-1127(00)00289-9.

Japan Meteorological Agency, 2017. Disaster Meteorological Report - Heavy Rain and Storms from 2016 August 16 to August 31 due to Typhoon No. 7, No. 9, No. 10, No. 11 and Front Line in 2016. Natural Disaster Report, Japan.

Kamimura, K., Kitagawa, K., Saito, S., Mizunaga, H., 2012. Root anchorage of hinoki (*Chamaecyparis obtuse (Sieb. Et Zucc.) Endl.*) under the combined loading of wind and rapidly supplied water on soil: analyses based on tree-pulling experiments. Eur. J. For. Res. 131, 219–227. https://doi.org/10.1007/s10342-011-0508-2.

Karizumi, N., 2010. The Latest Illustrations of Tree Roots. Seibundo Shinkosha Publishing Co., Ltd., Hongo Bunkyo-Ku, Tokyo.

Koizumi, A., 1987. Studies on the estimation of the mechanical properties of standing trees by non-destructive bending test. Res. Bull. Coll. Exp. For. Hokkaido Univ. 44, 1329–1415.

Koizumi, A. Motoyama, J., Sawata, K., Sasaki, Y., Hirai, T., 2010. Evaluation of drag

548 coefficients of poplar-tree crowns by a field test method. Journal of Wood Science. 56:3,
549 189-193. 10.1007/s10086-009-1091-8.
550 Kruse, F.A., Lefkoff, A.B., Boardman, J.W., Heidebrecht, K.B., Shapiro, A.T., Barloon, P.J.,
551 Goetz, A.F.H., 1993. The spectral image processing system (SIPS)-interactive
552 visualization and analysis of imaging spectrometer data. Remote Sens. Environ. 44, 145-
553 163. https://doi.org/10.1016/0034-4257(93)90013-N.
554 Kramer, M.G., Hansen, A.J., Taper, M.L., Kissinger, E.J., 2001. Abiotic controls on long-term
555 windthrow disturbance and temperate rain forest dynamics in southeast Alaska. Ecology
556 82, 2749–2768. https://doi.org/10.1890/0012-9658(2001)082[2749:ACOLTW]2.0.CO;2.
557 Krause, C., Lemay, A., Tremblay, S., Ruel, J.C., Plourde, P.Y., 2014. How does the root system
558 inhibit windthrow in thinned black spruce sites in the boreal forest? Trees 28, 1723–1735.
559 https://doi.org/10.1007/s00468-014-1080-4.
560 Kruse, F.A., Lefkoff, A.B., Boardman, J.W., Heidebrecht, K.B., Shapiro, A.T., Barloon, P.J.,
561 Goetz, A.F.H., 1993. The spectral image processing system (SIPS)—interactive
562 visualization and analysis of imaging spectrometer data. Remote Sens. Environ. 44, 145–
563 163. https://doi.org/10.1016/0034-4257(93)90013-N.
564 Lanquaye-Opoku, N., Mitchell, S.J., 2005. Portability of stand-level empirical windthrow risk
565 models. For. Ecol. Manag. 216, 134–148. https://doi.org/10.1016/j.foreco.2005.05.032.
566 Miller, K.F., Quine, C.P., Hunt, J., 1987. The assessment of wind exposure for forestry in Upland
567 Britain. For. Int. J. For. Res. 60, 179–192. https://doi.org/10.1093/forestry/60.2.179.
568 Mitchell, S.J., 2013. Wind as a natural disturbance agent in forests: a synthesis. For. Int. J. For.
569 Res. 86, 147–157. https://doi.org/10.1093/forestry/cps058.
570 Mitchell, S.J., Hailemariam, T., Kulis, Y., 2001. Empirical modeling of cutblock edge windthrow

risk on Vancouver Island, Canada, using stand level information. For. Ecol. Manag. 154, 117–130. https://doi.org/10.1016/S0378-1127(00)00620-4.

Mitchell, S.J., Ruel, J.C., 2015. Modeling windthrow at stand and landscape scales, in: Perera, A.H., Sturtevant, B.R., Buse, L.J. (Eds.), Simulation Modeling of Forest Landscape Disturbances. Springer International Publishing, Cham, pp. 17–43.

Morimoto, J., Nakagawa, K., Takano, K.T., Aiba, M., Oguro, M., Furukawa, Y., Mishima, Y., Ogawa, K., Ito, R., Takemi, T., Nakamura, F., Peterson, C.J., 2019. Comparison of vulnerability to catastrophic wind between *Abies* plantation forests and natural mixed forests in northern Japan. For. Int. J. For. Res. 92, 436–443. https://doi.org/10.1093/forestry/cpy045.

Murakami, H., Wang, Y., Yoshimura, H., Mizuta, R., Sugi, M., Shindo, E., Adachi, Y., Yukimoto, S., Hosaka, M., Kusunoki, S., 2012. Future changes in tropical cyclone activity projected by the new high-resolution MRI-AGCM. J. Clim. 25, 3237–3260. https://doi.org/10.1175/JCLI-D-11-00415.1.

Nakashizuka, T., 1989. Role of uprooting in composition and dynamics of an old-growth forest in Japan. Ecology 70, 1273–1278. https://doi.org/10.2307/1938186.

Nayak, S., Takemi, T., 2019a. Dynamical downscaling of Typhoon Lionrock (2016) for assessing the resulting hazards under global warming. J. Meteorol. Soc. Jpn. 97, 69–88. https://doi.org/10.2151/jmsj.2019-003.

Nayak, S., Takemi, T., 2019b. Quantitative estimations of hazards resulting from Typhoon Chanthu (2016) for assessing the impact in current and future climate. Hydrol. Res. Lett. 13, 20–27. https://doi.org/10.3178/hrl.13.20.

Oppenheimer, M., Campos, M., Warren, R., Birkmann, J., Luber, G., O'Neill, B., Takahashi, K.,

Berkhout, F., Dube, P., Foden, W., Greiving, S., Hsiang, S., Johnston, M., Keller, K., Kleypas, J., Kopp, R., Licker, R., Peres, C., Price, J., Robock, A., Schlenker, W., Stepp, J.R., Tol, R., van Vuuren, D., 2014. Emergent risks and key vulnerabilities, in: Field, C.B., Barros, V.R., Dokken, D.J., Mach, K.J., Mastrandrea, M.D., Bilir, T.E., Chatterjee, M., Ebi, K.L., Estrada, Y.O., Genova, R.C., Girma, B., Kissel, E.S., Levy, A.N., MacCracken, S., Mastrandrea, P.R., White, L.L. (Eds.), Climate Change 2014 Impacts, Adaptation, and Vulnerability Part A: Global and Sectoral Aspects Working Group II Contribution to the Fifth Assessment Report of the Intergovernmental Panel on Climate Change. Cambridge University Press, Cambridge, United Kingdom and New York, NY, USA, pp. 1039–1100.

Peterson, C.J., Pickett, S.T.A., 1991. Treefall and resprouting following catastrophic windthrow in an old-growth hemlock-hardwoods forest. For. Ecol. Manag. 42, 205–217. https://doi.org/10.1016/0378-1127(91)90025-Q.

Planet Lab Inc., 2020. PLANET IMAGERY AND ARCHIVE [WWW Document]. https://www.planet.com/products/planet-imagery/ (accessed 7.3.20).

QGIS Development Team, 2018. QGIS geographic information system. Open Source Geospatial Foundation Project. http://qgis.osgeo.org (accessed 29 May 2020).

QGIS.org, 2020. QGIS Geographic Information System [WWW Document]. Open Source Geospatial Found. Proj. https://www.qgis.org (accessed 13 July 2020).

Quine, C.P., Gardiner, B.A., 2007. Understanding how the interaction of wind and trees results in windthrow, stem breakage, and canopy gap formation, in: Johnson, E.A., Miyanishi, K. (Eds.), Plant Disturbance Ecology. Academic Press, Burlington, pp. 103–155.

Sandri, M., Zuccolotto, P., 2006. Variable selection using random forests. In Data Analysis,

Classification and the Forward Search: Proceedings of the Meeting of the Classification and Data Analysis Group (CLADAG) of the Italian Statistical Society, University of Parma, June 6–8, 2005. Zani S., Cerioli A., Riani M. and Vichi M. (eds). Springer Berlin 587 Heidelberg, pp. 263–270.

Strobl, C., Boulesteix, A.-L., Zeileis, A., Hothorn, T. 2007. Bias in random forest variable importance measures: illustrations, sources and a solution. BMC Bioinformatics. 8:1, 25. doi:10.1186/1471-2105-8-25.

Rentch, J., 2010. Relationship between treefall direction, slope-aspect, and wind in eight old-growth oak stands in the central hardwood forest, USA. J. Torrey Bot. Soc. 137, 391–400. https://doi.org/10.2307/25790860.

Ruel, J.C., Pin, D., Cooper, K., 1998. Effect of topography on wind behaviour in a complex terrain. For. Int. J. For. Res. 71, 261–265. https://doi.org/10.1093/forestry/71.3.261.

Schulzweida, U., 2019. CDO User Guide (Version 1.9.8). https://doi.org/10.5281/zenodo.3539275.

Shibuya, M., Urata, T., Torita, H., Iijima, H., 2011. Windthrow damage and tree shape in coniferous plantations in central Hokkaido, northern Japan. Jpn. J. For. Environ. 53, 53–59. https://doi.org/10.18922/jjfe.53.2_53.

Skamarock, W.C., Klemp, J.B., Jimy, D., David, O.G., Dale, B., Michael, G.D., Xiang-Yu, H., Wei, W., Jordan, G.P., 2008. Description of the Advanced Research WRF Version 3 (No. NCAR/TN-475+STR). University Corporation for Atmospheric Research.

Stathers, R.J., Rollerson, T.P., Mitchell, S.J., 1994. Windthrow Handbook for British Columbia Forests. Working Paper No. 9401. British Columbia Ministry of Forests, Victoria.

Takemi, T., 2019. Impacts of global warming on extreme rainfall of a slow-moving typhoon: a

case study for Typhoon Talas (2011). SOLA 15, 125–131. https://doi.org/10.2151/sola.2019-023.

Takemi, T., Ito, R., 2020. Benefits of high-resolution downscaling experiments for assessing strong wind hazard at local scales in complex terrain: a case study of Typhoon Songda (2004). Prog. Earth Planet. Sci. 7, 1–16. https://doi.org/10.1186/s40645-019-0317-7.

Yamamoto, S.I., 1989. Gap dynamics in climaxFagus crenata forests. Bot. Mag. Shokubutsu-Gaku-Zasshi 102, 93–114. https://doi.org/10.1007/BF02488116.